JACS
JOURNAL OF THE AMERICAN CHEMICAL SOCIETY
Article
pubs.acs.org/JACS

Facile Rearrangement of 3-Oxoalkyl Radicals is Evident in Low-Temperature Gas-Phase Oxidation of Ketones

Adam M. Scheer,*[,†] Oliver Welz,[†] Darryl Y. Sasaki,[‡] David L. Osborn,[†] and Craig A. Taatjes*[,†]

[†]Combustion Research Facility, Sandia National Laboratories, MS 9055, Livermore, California 94551, United States
[‡]Biological and Materials Science, Sandia National Laboratories, MS 9292, Livermore, California 94551, United States

Supporting Information

ABSTRACT: The pulsed photolytic chlorine-initiated oxidation of methyl-*tert*-butyl ketone (MTbuK), di-*tert*-butyl ketone (DTbuK), and a series of partially deuterated diethyl ketones (DEK) is studied in the gas phase at 8 Torr and 550−650 K. Products are monitored as a function of reaction time, mass, and photoionization energy using multiplexed photoionization mass spectrometry with tunable synchrotron ionizing radiation. The results establish that the primary 3-oxoalkyl radicals of those ketones, formed by abstraction of a hydrogen atom from the carbon atom in γ-position relative to the carbonyl oxygen, undergo a rapid rearrangement resulting in an effective 1,2-acyl group migration, similar to that in a Dowd−Beckwith ring expansion. Without this rearrangement, peroxy radicals derived from MTbuK and DTbuK cannot undergo HO_2 elimination to yield a closed-shell unsaturated hydrocarbon coproduct. However, not only are these coproducts observed, but they represent the dominant oxidation channels of these ketones under the conditions of this study. For MTbuK and DTbuK, the rearrangement yields a more stable tertiary radical, which provides the thermodynamic driving force for this reaction. Even in the absence of such a driving force in the oxidation of partially deuterated DEK, the 1,2-acyl group migration is observed. Quantum chemical (CBS-QB3) calculations show the barrier for gas-phase rearrangement to be on the order of 10 kcal mol^{-1}. The MTbuK oxidation experiments also show several minor channels, including β-scission of the initial radicals and cyclic ether formation.

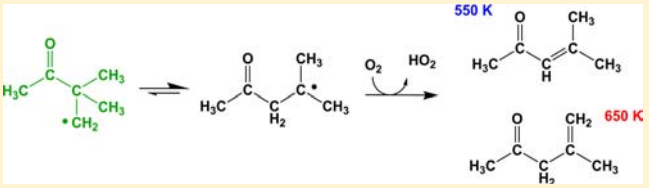

1. INTRODUCTION

Radical rearrangement isomerizations play vital roles in a wide range of important chemical schemes including pyrolysis,[1−3] oxidation,[4,5] and synthesis.[6,7] A large variety of radical rearrangements have been observed in both the liquid[6−9] and gas phases.[4,5] A thorough understanding of these reactions is necessary to build accurate kinetic models to describe complex oxidation and ignition schemes. Furthermore, radical rearrangement reactions, both unanticipated[9] and by design,[6] play important roles in many synthetic schemes. In this study, we report that one such radical rearrangement, a 1,2-acyl group migration well-known in solution,[10] is prominent in the gas-phase oxidation of branched ketones. We have investigated the low-temperature oxidation of ketones because they are among the organic compounds produced from conversion of lignocellulose by endophytic fungi and have potential application as biofuels.[11−13] However, the fundamental chemistry related to their autoignition is not well studied.

Scheme 1 depicts the 1,2-acyl group migration investigated in this work. A primary carbon-centered radical, with the radical site initially at the γ position relative to the carbonyl oxygen, attacks the carbonyl carbon atom (C_α), which leads to a cyclic transition-state structure. Fission of the C_α−C_β bond exchanges the C_β and C_γ atoms. Depending on the nature of the β-carbon substituent groups, this rearrangement can yield a primary radical ($R_{1,2}$ = H) or a more stable secondary (R_1 = alkyl group, R_2 = H) or tertiary ($R_{1,2}$ = alkyl group) radical. A thermodynamic driving force for the isomerization exists if the final radical site has a higher degree of substitution than the initial radical site.

Such a rearrangement was observed in solution as early as 1961,[14] and a general description was given by Karl et al.[15] in 1972. In that work, the authors studied a series of perlevulinate esters. Upon thermal decomposition, the esters were designed to give a primary radical such as the reactant in Scheme 1. Hydrogen-donating solvents were used to terminate the reaction, and products were identified using gas−liquid chromatography. The rearrangement was found to occur rapidly, as only trace amounts of products expected from the initial primary radical were observed. A significant driving force was apparent for the forward reaction if the R_1 and R_2 substituents stabilized the final product of the rearrangement reaction. The authors deduced that the cyclopropoxy radical is not a discrete intermediate of the reaction and rather suggested that a cyclic

Scheme 1

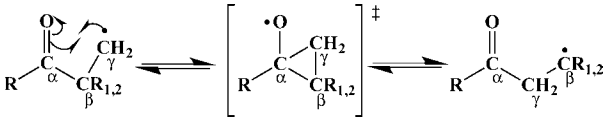

Received: June 12, 2013
Published: August 23, 2013

dx.doi.org/10.1021/ja405892y | J. Am. Chem. Soc. 2013, 135, 14256−14265

Scheme 2

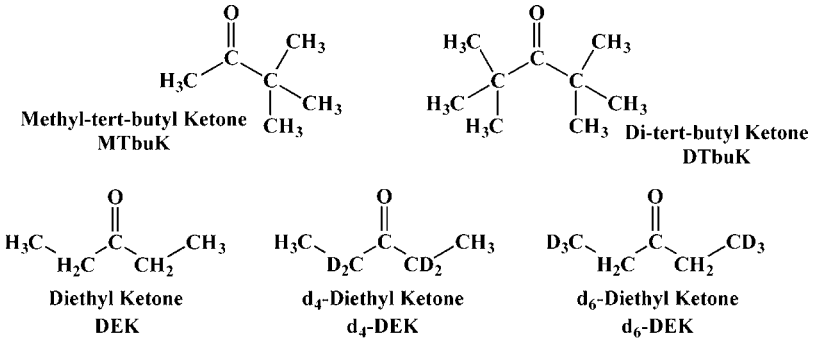

Scheme 3

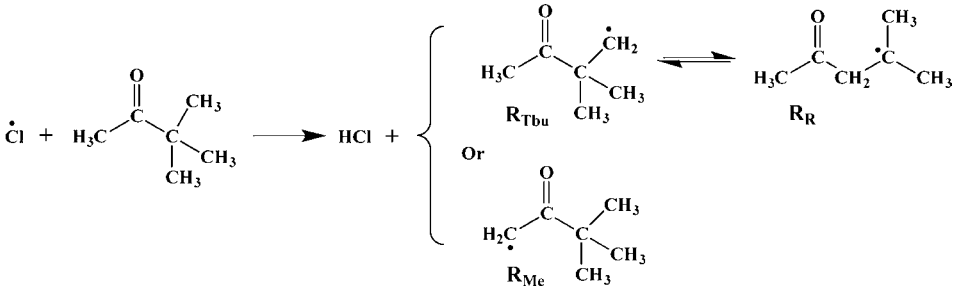

transition state exists with radical character at both carbon atom radical centers. Such a rearrangement was also later exploited in the development of the Dowd−Beckwith ring expansion for synthesis of cyclic ketones.[6,16,17] Calculations of the mechanism of this rearrangement support a concerted rearrangement via a cyclic transition-state structure.[18,19] Moreover, kinetics experiments[20−22] show that the rearrangement is rapid, with A-factors in excess of 10^{10} s^{-1} and activation energies (in solution) on the order of 10 kcal mol^{-1} or less. Calculations for the rearrangements predict a relatively small change in the Gibbs free activation energy upon solution ($\Delta\Delta G$),[19] suggesting rapid gas-phase 1,2-acyl group shifts as well. However, some calculations[18] of acyl-shift rearrangement show substantially higher barriers, in excess of 20 kcal mol^{-1}, large enough to limit the role of such isomerizations in low-temperature gas-phase oxidation.

In this work, we demonstrate that such rearrangements are indeed facile in the gas phase and that they play an important role in the gas-phase low-temperature oxidation of ketones, specifically methyl-*tert*-butyl ketone (3,3-dimethyl-2-butanone, MTbuK) and di-*tert*-butyl ketone (2,2,4,4-tetramethylpentan-3-one, DTbuK). Using partially deuterated diethyl ketones (pentan-3-one, DEK), we show that this rearrangement is also active in DEK, even without any thermodynamic driving force. The ketones studied are shown in Scheme 2. These compounds serve as prototypes to establish chemical oxidation mechanisms important for families of larger ketones. CBS-QB3 quantum chemical calculations of barrier heights for the 1,2-acyl group migration support the mechanism. In addition, stationary points on the potential energy surfaces for the reactions of the MTbuK radicals with O_2 are calculated to elucidate product formation channels relevant to the overall gas-phase oxidation.

Low-temperature oxidation of these ketones was investigated by using pulsed photolytic chlorine atom initiation at 8 Torr and 550 and 650 K in the presence of a large excess of O_2. Reactions 1 and 2 show the general Cl-initiated oxidation reactions. A Cl· atom produced by 351 nm photolysis of Cl_2 abstracts an H-atom from the ketone molecule RH to generate an initial ketonyl (i.e., oxoalkyl) radical R.[23] The radical R can then either undergo unimolecular reactions or add O_2 in a barrierless or near barrierless reaction[5,24] to form a peroxy radical RO_2, which then reacts further to yield products.

$$\dot{Cl} + R{-}H \rightarrow R + HCl \quad (1)$$

$$R + O_2 \rightleftharpoons RO_2 \rightarrow \text{Products} \quad (2)$$

Reaction of Cl· with MTbuK (see Scheme 3) yields two distinct initial radicals: a primary radical R_{Tbu} (2,2-dimethyl-3-oxobutyl) resulting from abstraction of an H-atom from the *tert*-butyl group and a primary radical R_{Me} (3,3-dimethyl-2-oxobutyl) resulting from H-abstraction from the methyl group bound to C_α. R_{Tbu} can rearrange via an effective 1,2 acyl group shift as shown in Scheme 1, which would yield a more stable tertiary radical R_R (2-methyl-4-oxopent-2-yl). The radical abbreviations introduced in Scheme 3 will be used throughout the text.

Kaiser et al.[25] report rate constants for the reaction of Cl· with butanone of 2.3×10^{-11} exp(−1.8 kcal mol^{-1}/RT) cm^3 s^{-1} to form HCl + 2-oxobutyl and 1.9×10^{-11}exp(−0.47 kcal mol^{-1}/RT) cm^3 s^{-1} to form HCl + 3-oxobutyl. These rate constants allow an estimate for the ratio of R_{Tbu} to R_{Me} (Scheme 3) expected in this work. The additional methyl groups in MTbuK are not expected to have major impact on the per-hydrogen rates of H-abstraction from the 1 or 4 positions. Using the above rate constants and normalizing to account for the number of chemically equivalent hydrogen atoms, the ratio of R_{Tbu}/R_{Me} is predicted to be 8.4 at 550 K and 6.9 at 650 K.

Among the important typical unimolecular reactions of RO_2 is the elimination of HO_2, which yields an unsaturated, closed-shell hydrocarbon byproduct.[5,26−29] An example of such a reaction is shown in reaction 3 for the addition of O_2 to the *n*-propyl radical followed by the elimination of HO_2 to yield propene.[30] The HO_2 elimination requires that at least one of

dx.doi.org/10.1021/ja405892y | J. Am. Chem. Soc. 2013, 135, 14256−14265

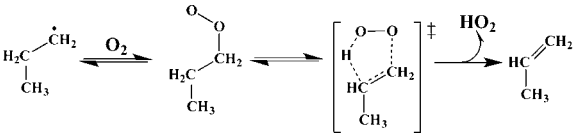

(3)

the carbon atoms in the β position to the peroxy group is also bound to at least one H-atom.

Because neither the HO_2 radical nor the unsaturated byproduct is very reactive in low-temperature autoignition schemes, channels such as reaction 3 are effectively 'chain-terminating' for autoignition.[5] In the case of MTbuK and DTbuK, every carbon atom in the alkyl branches is either quaternary or associated with a terminating methyl group. Therefore, in the absence of radical rearrangement reactions, no HO_2-elimination pathways analogous to reaction 3 are available for oxidation of these ketones. If, however, the radical rearrangement reaction of Scheme 1 is competitive with O_2 addition to the initial radical, distinct coproducts following HO_2 elimination would be expected from oxidation of R_R.

2. EXPERIMENT

The fundamental oxidation chemistry of the ketones was studied using multiplexed photoionization mass spectrometry (MPIMS) with tunable vacuum ultraviolet (VUV) synchrotron ionizing radiation at the Advanced Light Source (ALS) of Lawrence Berkeley National Laboratory. The experiment has been described in detail previously,[31,32] and only a brief synopsis will be given here. The apparatus consists of a heated 1.05 cm i.d. quartz flow tube with a ~650 μm aperture in the sidewall through which gas escapes. The effluent gas is collimated into a molecular beam by passing through a 1.5 mm diameter skimmer into a differentially pumped ionization chamber. Quasi-continuous, tunable ionizing VUV radiation provided by the ALS synchrotron intersects the molecular beam orthogonally, and the ions that are formed are collimated and accelerated into an orthogonal acceleration linear time-of-flight mass spectrometer. Products are detected as a function of mass, time, and photon energy yielding a 3-dimensional data set that can be sliced and integrated to obtain photoionization spectra and temporal profiles for individual species.[32] Comparison of the photoionization spectrum of a product mass channel with the calibration spectra of pure compounds at a particular mass allows the identification and quantification of products at an isomer-resolved level.[31,32]

The ketone is introduced either via helium flow through a bubbler held at 20 °C or via a prepared mixture of the sample in He. Ketone densities of (2−7) × 10^{13} cm^{-3} are used. Photolysis of Cl_2 by a pulsed excimer laser operating at 351 nm and 4 Hz yields an initial Cl atom concentration between 2 × 10^{12} and 9 × 10^{12} cm^{-3}. The ratio of $[Cl]_0/[RH]_0$ is maintained at ~0.1. The reaction proceeds in a large excess of O_2 (2.5 × 10^{16} cm^{-3}). The averaged prephotolysis signal is subtracted, resulting in difference mass spectra that show positive signals for products generated by the photolytically initiated reactions. Signals are normalized to the ionizing photon flux. Calibrated mass flow controllers are used to introduce reactants and carrier gas into the flow tube. The pressure in the tube is maintained at 8 Torr by feedback control of a butterfly valve in the exhaust line.

MTbuK, DTbuK, and diisopropyl ketone were obtained commercially at stated purities of 98%. The nondeuterated diethyl ketone was obtained commercially at a stated purity of >99%. The d_4- and d_6-diethyl ketone isotopologs were obtained commercially and were assayed at 99.8% and 99.6% chemical purity, respectively. Mesityl oxide was obtained commercially at a purity of >95%. The major impurity is the isomesityl oxide isomer. A modified literature procedure[33,34] was followed to synthesize a pure sample of isomesityl oxide. Details of the synthesis are given in the Supporting Information. 2,5-dimethylcyclopentanone and 2,2,5,5-tetramethylcyclopentanone were obtained commercially at stated purities of 98%. All samples were freeze−pump−thawed before use.

3. RESULTS AND DISCUSSION

3.1. HO_2-Elimination Channels at 550 K.

3.1.1. MTbuK. Figure 1a shows the product mass spectrum for the Cl-initiated

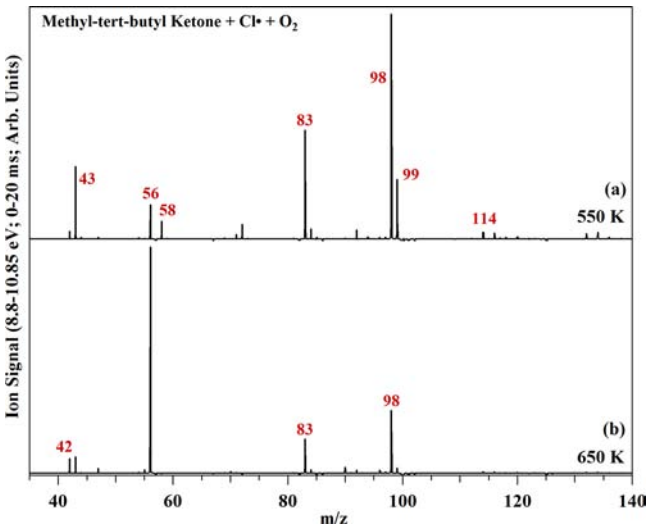

Figure 1. Difference mass spectra of Cl-initiated oxidation of MTbuK at (a) 550 and (b) 650 K from integrating the ion signal for the 20 ms time frame immediately following photolysis and over ionizing photon energies from 8.0 to 10.5 eV. Averaged background signal before photolysis has been subtracted, and negative signal arising from consumption of MTbuK is omitted for clarity.

oxidation of MTbuK ($C_6H_{12}O$) at 550 K and 8 Torr in the presence of 2.5 × 10^{16} cm^{-3} (~18 mol %) O_2. The negative signal arising from reactive removal of MTbuK (m/z = 100) and its fragment ions (m/z = 86, m/z = 82 and m/z = 57) is not shown in this spectrum. At 550 K, the dominant product peaks observed are at m/z = 98 and 83. The m/z = 98 ($C_6H_{10}O$) peak corresponds to the stable coproducts of HO_2 loss from RO_2, whereas m/z = 83 is assigned as a fragment ion that arises from dissociative ionization of $C_6H_{10}O$ neutrals. Reaction 4 shows the 1,2-acyl group migration of R_{Tbu} followed

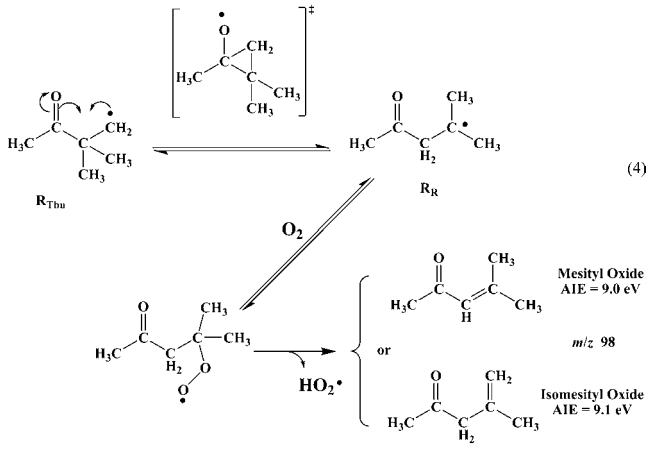

(4)

by O_2 addition to R_R and the expected products from subsequent HO_2 elimination, mesityl oxide (4-methyl-pent-3-en-2-one) and isomesityl oxide (4-methylpent-4-en-2-one), along with their calculated adiabatic ionization energies (AIEs) at the CBS-QB3 level.[35,36]

dx.doi.org/10.1021/ja405892y | J. Am. Chem. Soc. 2013, 135, 14256−14265

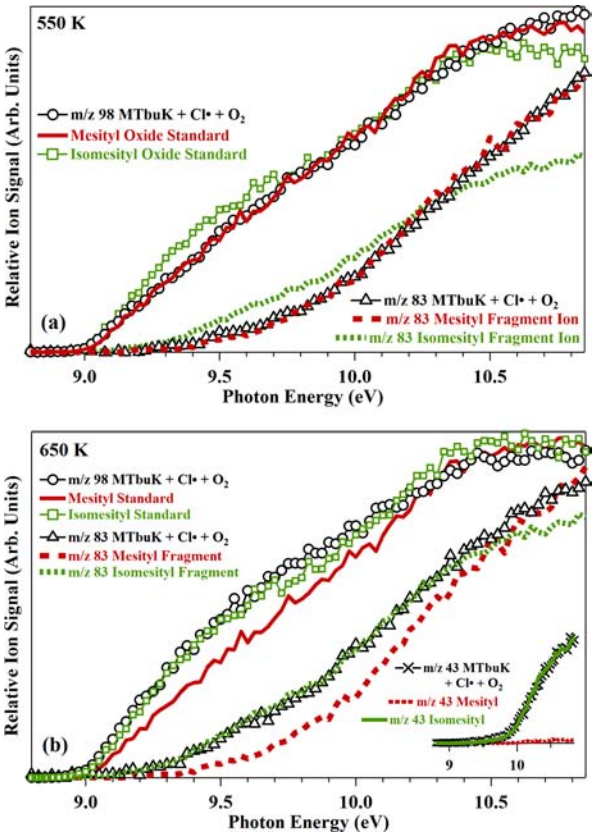

Figure 2. Comparison of the photoionization spectra for the m/z = 98 peak observed in Cl-initiated oxidation of MTbuK at (a) 550 and (b) 650 K with the mesityl oxide and isomesityl oxide calibration spectra. The indicated fragment ion spectra resulting from dissociative photoionization of mesityl oxide and isomesityl oxide are also shown. The mesityl oxide and isomesityl oxide calibration spectra were taken at 550 K.

Figure 2a compares the photoionization spectra at 550 K associated with the m/z = 98 and 83 peaks with the photoionization spectra of the parent ions of mesityl oxide and isomesityl oxide at m/z = 98 and their respective m/z = 83 fragment ions. The mesityl oxide spectra match the corresponding product spectra in MTbuK oxidation at 550 K nearly exactly. Similarly, one can see the isomesityl oxide and fragment ion curves poorly match the 550 K product spectra. An upper bound of 20% for the isomesityl oxide contribution at 550 K is estimated from a least-squares fitting procedure in which the mesityl oxide and isomesityl oxide absolute photoionization spectra are taken as basis functions for the m/z = 98 product photoionization spectrum.[37] These results, in combination with the product branching ratios discussed below, establish HO_2 elimination as the dominant channel in MTbuK oxidation at 550 K. Therefore the gas-phase 1,2-acyl group migration is fast relative to O_2 addition (which occurs with a pseudo-first order rate coefficient on the order of 10^5 s^{-1} at the conditions of this work). Figure 1b shows the product mass spectrum for MTbuK oxidation at 650 K. At this temperature, β-scission channels of the initial radicals become important relative to oxidation channels. This change is reflected by the growth of the isobutene peak (m/z = 56). Other products observed in MTbuK oxidation will be discussed below.

Figure 3 shows stationary points on the potential energy surface calculated for O_2 addition to the unrearranged (R_{Tbu}) and rearranged (R_R) radicals from MTbuK. The calculations were performed with Gaussian 09[38] using the CBS-QB3 composite method.[35,36] The barrier for the 1,2-acyl group migration ($R_{Tbu} \rightarrow R_R$) is calculated to be 9.1 kcal mol^{-1}. This value is far smaller than the isomerization barrier (~20 kcal mol^{-1}) calculated with MP2 or MP3 methods for rearrangement of the unsubstituted (2-oxocyclopentyl)methyl radical[18] but is similar to the barrier (9.5 kcal mol^{-1}) calculated[19] in a Dowd–Beckwith expansion of the methyl 1-methyl-2-oxocyclopentane-1-carboxylate. A single-point

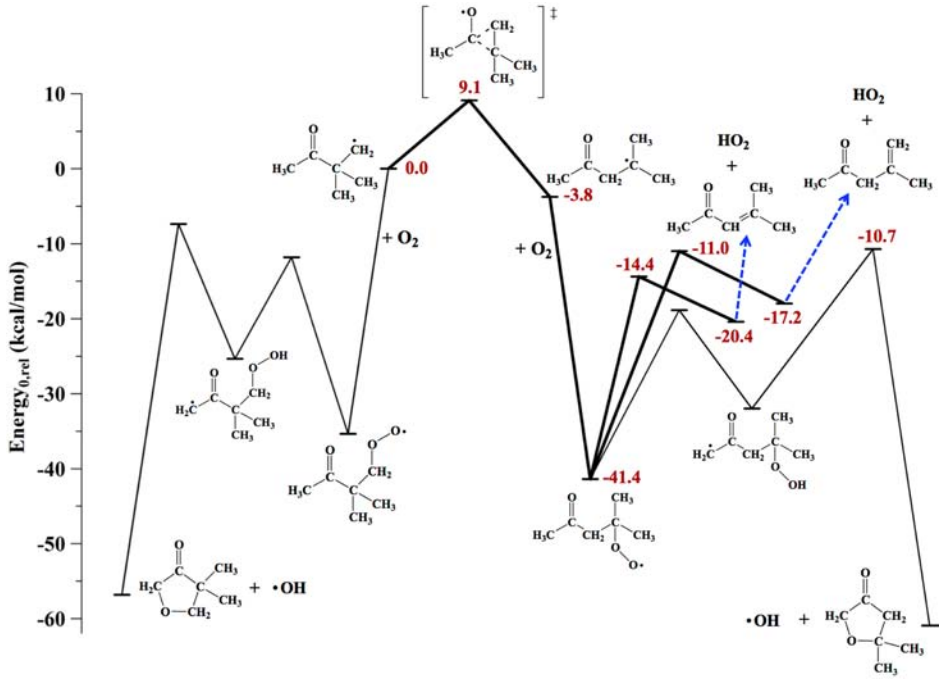

Figure 3. Stationary points on the potential energy surface for reaction of O_2 with the MTbuK radicals, R_{Tbu} and R_R. Energies at 0 K are calculated at the CBS-QB3 level. Several β-scission channels are also possible but for clarity are not included.

dx.doi.org/10.1021/ja405892y | J. Am. Chem. Soc. 2013, 135, 14256–14265

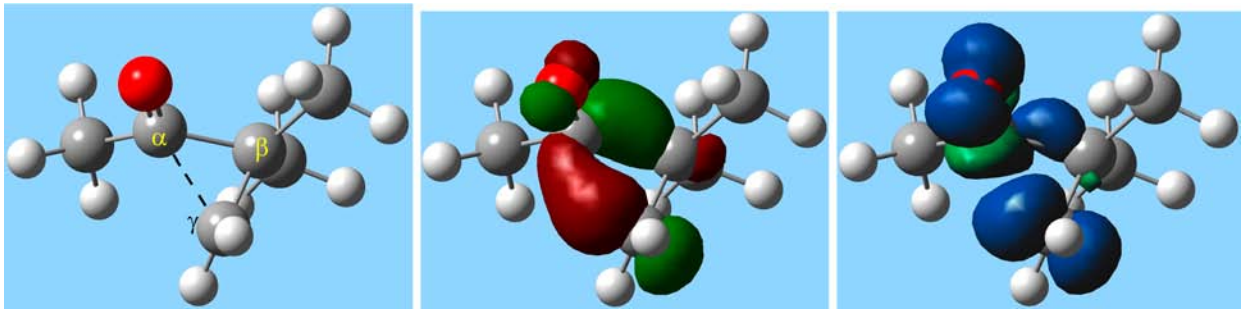

Figure 4. Left: Geometry at the saddle point associated with the 1,2-acyl group migration reaction for the initial R_{TBu} radical of MTbuK (2,2-dimethyl-3-oxobutyl) calculated at the B3LYP/6-311G(d,p) level of theory. Middle: HOMO calculated at the saddle point (isovalue = 0.08). Right: Spin density calculated at the saddle point (isovalue = 0.01) resulting from the same calculation.

energy calculation at the CCSD/6-31G(d) level was carried out to investigate the extent of multireference character at the ($R_{Tbu} \rightarrow R_R$) saddle point. A value of 0.0197 was obtained for the T1 diagnostic formulated by Lee et al.,[39] within the range in which the use of single-reference methods is appropriate. The geometry at this saddle point is given in Table S1. The resulting R_R radical is calculated to be more stable than R_{Tbu} by 3.8 kcal mol^{-1} (with similar entropy), sufficient to shift the equilibrium to favor R_R by >30:1 at 550 K. After rearrangement and O_2 addition, the lowest-energy unimolecular reaction pathway for the resulting R_RO_2 is HO_2 elimination to form mesityl oxide, in accord with the experimental observations. Both the barrier and product energies are calculated to be ~3 kcal mol^{-1} higher for isomesityl oxide formation. These HO_2-elimination channels are shown in bold. Other channels in Figure 3 are discussed below.

The geometry of the saddle point for the 1,2-acyl group migration is shown in Figure 4, along with the orbital diagram for the highest (singly) occupied molecular orbital (HOMO) and the spin density plot (the molecular orientation in all diagrams is equivalent). The HOMO at the saddle point contains significant bonding character between both the α and β carbons and the α and γ carbons. Similarly, these regions contain a high degree of spin density, suggesting the unpaired electron resides both at the initial and final radical sites. Efforts to locate a distinct cyclopropoxy radical intermediate failed, tending to confirm that a discrete cyclic intermediate is not involved in the reaction when stabilizing substituents are present at C_β and that the rearrangement rather occurs over a single barrier, as suggested by Karl et al.,[15] and noted in other calculations of similar rearrangements.[18] Because the configuration at the saddle point involves radical character at both the β and γ carbons, a larger degree of alkyl substitution at the initial β site is indeed expected to facilitate isomerization.

The CBS-QB3 calculations for the simplest case of this rearrangement, the reversible ring-opening of the cyclopropoxy radical, provide a useful comparison. The distribution of electronic spin density at the saddle point for cyclopropoxy ring-opening is completely analogous to that shown in Figure 4. Ring closure of 3-oxopropyl to cyclopropoxy has a barrier of 11.2 kcal mol^{-1}. The electronic energy of the cyclopropoxy radical is <0.25 kcal mol^{-1} below the electronic energy of the saddle point leading to ring-opening. When including zero-point corrections, the energy of cyclopropoxy is 0.5 kcal mol^{-1} *above* the saddle point energy, which implies the cyclopropoxy radical is essentially unbound. The $R_{Tbu} \rightarrow R_R$ reaction associated with MTbuK has a lower barrier of 9.1 kcal mol^{-1}, and no stable cyclic intermediate is found. These observations are consistent with the stabilization of the cyclic structure expected from substituents at the β carbon.

3.1.2. DTbuK. Observation of an analogous 1,2-acyl group migration would be expected in the Cl-initiated oxidation of DTbuK. In fact, this rearrangement was studied by Ingold and co-workers,[21] who measured a rate coefficient in CCl_4 solution of 8.7×10^{10} exp(−7.77 kcal mol^{-1}/RT) s^{-1}. Even if the activation energy in the gas phase is several kcal mol^{-1} larger, the rearrangement should compete with O_2 addition under the present conditions. The 550 K product mass spectrum for Cl-initiated oxidation of DTbuK ($C_9H_{18}O$, m/z = 142) indeed displays a strong signal from the product of HO_2 elimination at m/z = 140 ($C_9H_{16}O$) as well as a corresponding fragment ion at m/z = 83, analogous to that from mesityl oxide ionization (see reactions S2 and S3). The respective photoionization spectra are shown in Figure 5a along with the time traces in Figure 5b. Scheme 4 shows the expected products of HO_2 elimination for DTbuK oxidation after the 1,2-acyl group migration in analogy to MTbuK (reaction 4). These products were not commercially available nor did we attempt to synthesize them. However, the calculated AIEs of both species are in good agreement with the observed ionization onset of 8.7 eV in the m/z = 140 product spectrum.

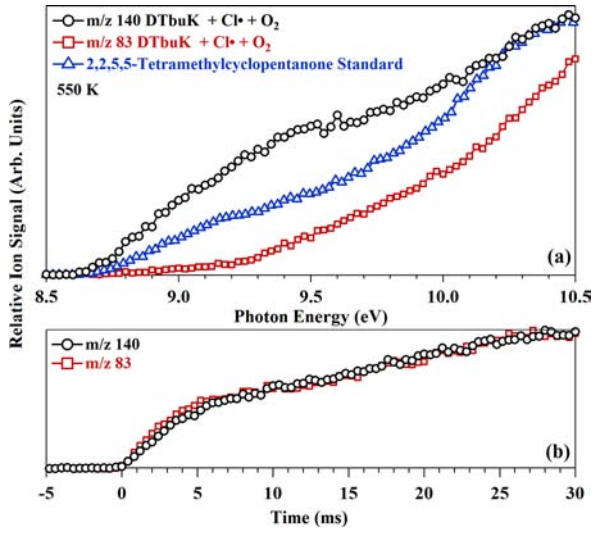

Figure 5. (a) Photoionization spectra for the m/z = 140 peak observed in Cl-initiated oxidation of DTbuK at 550 K and for a 2,2,5,5-tetramethylcyclopentanone standard. (b) Time traces of the m/z = 140 product of HO_2-elimination and its m/z = 83 fragment ion in DTbuK oxidation.

dx.doi.org/10.1021/ja405892y | J. Am. Chem. Soc. 2013, 135, 14256−14265

Scheme 4

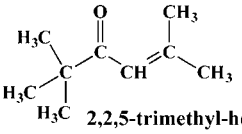

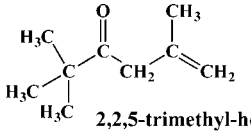

An alternative pathway, as shown in reaction 5, involves a ring closure upon ejection of HO_2 via the peroxy radical formed

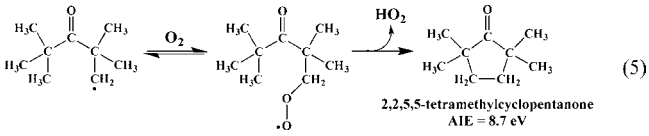

(5)

by O_2 addition to the initial DTbuK radical without acyl migration. Such a reaction would yield 2,2,5,5-tetramethylcyclopentanone. Similarly, a ring closure to form a three-membered ring could also be possible but would be high in energy and therefore not expected.

The measured photoionization spectrum of 2,2,5,5-tetramethylcyclopentanone (m/z = 140) is given in Figure 5a. Though its ionization onset matches the observed onset of the m/z = 140 product spectrum of DTbuK oxidation, the shapes of the curves clearly disagree. However, it is possible that two or more isomers may contribute to the m/z = 140 product photoionization spectrum, and the onset of the 2,2,5,5-tetramethylcyclopentanone photoionization spectrum does not exclude it from consideration. The 1,2-acyl group migration would also be expected in diisopropyl ketone and an analogous reaction to eq 5 would yield 2,5-dimethylcyclopentanone. Figure S1 shows the ionization onset of 2,5-dimethylcyclopentanone occurs below the photon energy of the m/z = 112 product of HO_2 elimination in diisopropyl ketone, providing strong evidence that such ring-closing channels are unimportant.

3.1.3. DEK. Unlike MTbuK and DTbuK, the initial primary 3-oxopentyl radical derived from H-abstraction at the methyl group of DEK does not have a thermodynamic driving force favoring the 1,2-acyl group migration, as the rearrangement of this radical regenerates the same species (reaction 6a). The

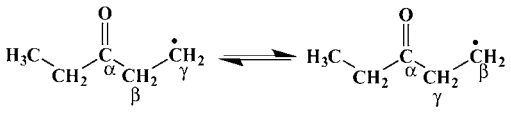

(6a)

CBS-QB3 calculations on reaction 6a do show a stable cyclic intermediate as well as two (symmetric) saddle points for ring closure and ring opening, with a barrier height of 11.2 kcal mol^{-1} above the initial 3-oxopentyl radical. Selectively deuterating either the β (d_4-DEK) or γ (d_6-DEK) sites yields a molecule that can give distinct products depending on rearrangement (see reactions 6b and 6c).

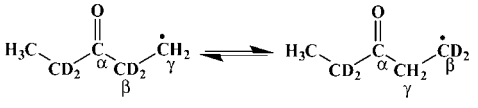

(6b)

From reactions 6b and 6c, it can be seen that HO_2 elimination from the primary radical of d_4- and d_6-DEK would yield vinyl ethyl ketone (1-penten-3-one, VEK) at different masses depending on whether HO_2 elimination originates from the original or rearranged radical. These pathways are depicted in Scheme 5 for both molecules, with the rearranged radical pathway in the right column.

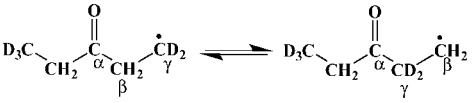

(6c)

Chlorine atom reaction with undeuterated DEK is expected to yield the primary DEK radical and the secondary DEK radical (3-oxopent-2-yl) in a ratio of approximately 1:1 at 550 K.[40] In the case of the initial secondary radical, HO_2/DO_2 elimination will only yield one isotopolog for d_4- and d_6-DEK oxidation, which, as shown in reactions 7a and 7b, will yield VEK at the same value of m/z as would be observed for reaction of the initial (nonrearranged) primary radical (Scheme 5).

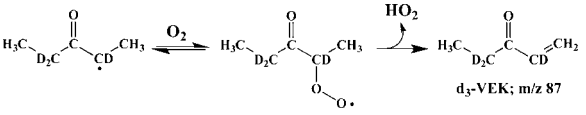

(7a)

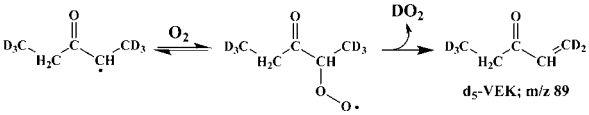

(7b)

Figure 6a shows the product mass spectra resulting from the 550 K Cl-initiated oxidation of DEK and d_4- and d_6-DEK in the range of the coproducts of HO_2/DO_2 elimination. Figure 6b compares the photoionization spectrum for VEK ($C_2H_5C(O)CHCH_2$; m/z = 84) plotted next to m/z = 84 from DEK oxidation, m/z = 87 and 88 from d_4-DEK, and m/z = 89 from d_6-DEK. These spectra are consistent with VEK (ionization onset 9.4 eV) as the principal HO_2-elimination product. The Figure 6b inset reveals a minor onset near 8.4 eV for m/z = 84 in DEK oxidation. This signal may be due to formation of a small amount of 3-hydroxy-penta-1,3-diene (AIE = 8.24 eV). The presence of this minor m/z = 84 product in the photoionization spectrum likely causes the slight vertical shift relative to the VEK standard for much of the spectrum. In addition to producing signal at its parent mass (m/z = 84), the VEK calibration spectrum also shows a small fragment ion signal at m/z = 83 and by analogy explains at least a portion of the m/z = 86 and 88 signal in d_4- and d_6-DEK oxidation, respectively.

The signal at m/z = 88 in d_4-DEK oxidation is too large to arise solely from the ^{13}C isotopolog of the m/z = 87 signal from d_3-VEK (Figure 6a) and is in very good agreement with the authentic VEK photoionization spectrum (Figure 6b). This excess signal is attributed to d_4-VEK from the rearrangement channel of Scheme 5. The relative amount of VEK resulting from rearrangement (observed at m/z = 88 for both initial isotopologs) is clearly less in d_6-DEK than in d_4-DEK (Figure 6a), because of kinetic deuterium isotope effects in the initial radical

dx.doi.org/10.1021/ja405892y | J. Am. Chem. Soc. 2013, 135, 14256−14265

Scheme 5

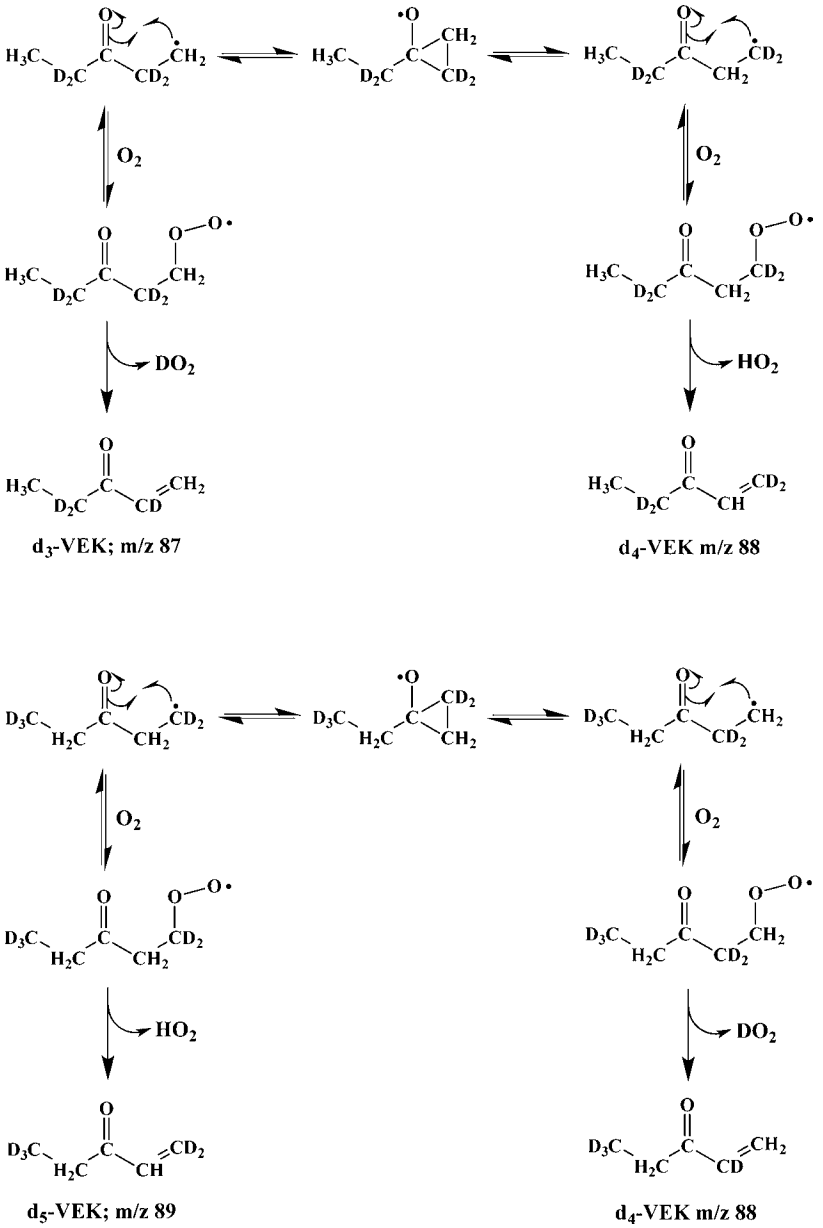

formation and in the HO_2 elimination. In d_6-DEK oxidation a preference of H- over D-atom abstraction will result in more initial production of the secondary radical, a species expected to only produce d_5-VEK (m/z = 89) via the associated HO_2-elimination channel. Furthermore, the RO_2 resulting from the rearranged primary radical,[41] allowing other channels such as cyclic ether formation[5] to become more competitive. In contrast, in d_4-DEK oxidation these kinetic isotope effects will favor VEK from the rearranged radical.

3.2. Other Product Channels in MTbuK Oxidation. To further support the prominence of HO_2 elimination from the reaction of the rearranged R_R radical with O_2 in MTBuK, we compare the yields of mesityl and isomesityl oxide to the yields of the other stable products observed. Table 1 gives branching ratios determined for the Cl-initiated oxidation experiments of this work at 550 and 650 K. The mesityl oxide product of HO_2 elimination (following O_2 addition to R_R) dominates at 550 K, accounting for ∼70% of the product distribution. Other channels, including β-scission reactions, which yield small molecule products, and the 'chain-propagating' formation of OH + cyclic ethers[5,24] (discussed below) are minor (but nonzero) at this temperature.

As discussed above, R_{Me} is expected to be a minor product of H-abstraction of MTbuK by Cl· (Scheme 3). Figure 7 shows the potential energy surface calculated for important channels anticipated for O_2 addition to R_{Me}. This radical shows vinoxy-type resonance stabilization. As a result, the associated RO_2 well is shallow (22 kcal mol^{-1}) relative to the entrance channel, so that the barriers to bimolecular products lie above the R + O_2 reactants, and the equilibrium of the R_{Me} + O_2 ↔ $R_{Me}O_2$ association reaction favors reactants even at a relatively low temperature.[5] In contrast, O_2 addition to either R_{Tbu} or R_R results in a much deeper RO_2 well (35−40 kcal mol^{-1}). With no likely rearrangement reactions and no neighboring C−H bonds, HO_2 elimination originating from the oxidation channels of R_{Me} is expected to be unimportant.

dx.doi.org/10.1021/ja405892y | J. Am. Chem. Soc. 2013, 135, 14256−14265

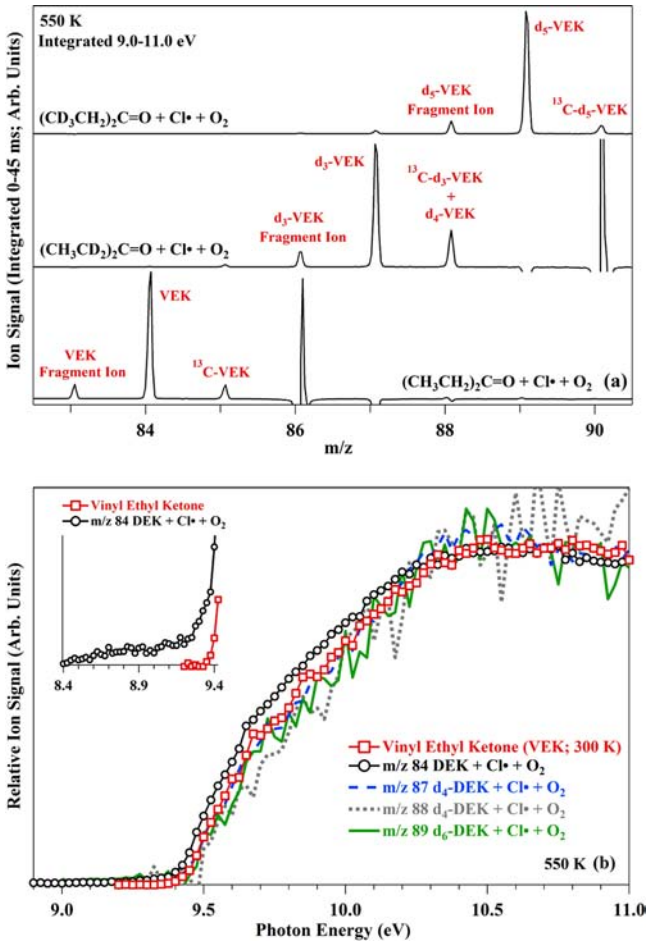

Figure 6. (a) Bottom: Product mass spectrum of Cl-initiated oxidation of DEK at 550 K normalized to photocurrent resulting from integrating the ion signal for the 45 ms time frame immediately following photolysis and over ionizing photon energies from 8.3 to 11.0 eV. Middle: Same for d_4-DEK integrated over 9.0−11.0 eV. Top: Same for d_6-DEK integrated over 9.0−11.0 eV. (b) Photoionization spectra for the indicated peaks observed in Cl-initiated oxidation of DEK and deuterated DEKs at 550 K along with that for a VEK standard.

Aside from HO_2 elimination, a typical RO_2 species can undergo reversible isomerization to a hydroperoxyalkyl radical (QOOH) via internal H-abstraction. These QOOH radicals can eject an OH radical upon ring closure to form cyclic ethers.[5] Figures 3 and 7 show that QOOH → OH + dimethyldihydrofuran-3(2*H*)-one (m/z = 114) channels are available for the reaction of O_2 + R_{Me}, R_{Tbu}, and R_R. The feature at m/z = 114 in Figure 1a might arise from these products, i.e., 4,4-dimethyl-dihydrofuran-3(2*H*)-one and 5,5-dimethyldihydrofuran-3(2*H*)-one. Several three- and four-membered cyclic ether products are also possible but are less likely because they must follow higher energy pathways; we therefore did not include them in Figures 3 and 7. Figure 8 shows the m/z = 114 photoionization spectrum from MTbuK oxidation at 550 K. The adiabatic ionization energies calculated for the expected dimethyldihydrofuran-3(2*H*)-one products agree well with the observed ionization onset. Formation of 5,5-dimethyldihydrofuran-3(2*H*)-one from R_{Me} + O_2 requires a 1,2-acyl group migration in the resulting QOOH (Figure 7). This primary QOOH → tertiary QOOH isomerization occurs with a calculated barrier of 6.1 kcal mol^{-1} relative to the primary QOOH radical, 3.0 kcal mol^{-1} less than that calculated for R_{Tbu} ↔ R_R.

Table 1. Branching Ratios Determined for the Products of Cl-Initiated Oxidation of MTbuK at 550 and 650 K[a]

	m/z	assignment	energy (eV)	standard cross section (Mb)	branching ratio[e]
550 K	42	ketene	9.95	18.4	0.02[b]
	56	isobutene	9.375	3.93	0.11
	58	acetone	10.675	14.61	0.12
	98	mesityl oxide	9.5	8.39	0.71
	114	cyclic ether[c]	10.35	18[d]	0.03
650 K	42	ketene	9.95	18.4	0.04
	56	isobutene	9.375	3.93	0.74
	58	acetone	10.675	14.61	<0.01
	98	isomesityl oxide (0.75) + mesityl oxide (0.25)[f]	9.5	8.39	0.22
	114	cyclic ether	10.35	18[d]	<0.01

[a]Values result from integrating product signals over the 20 ms immediately following photolysis. Energies listed are the point at which the signal was compared with a standard. These energies vary to ensure fragment ions of the same m/z value are not incorporated into the measurement for a particular species. The photoionization cross sections from calibration spectra of the pure compounds ("standard cross sections") given are at the corresponding energies. [b]Due to uncertainty in the assignment, value is an upper bound. [c]Expected products are 4,4-dimethyl-tetrahydrofuran-3(2*H*)-one and 5,5-dimethyl-tetrahydrofuran-3(2*H*)-one. [d]Cross section is estimated. Error is expected to be ±50%. [e]Includes empirical correction for time-of-flight mass discrimination factor. [f]Branching ratio of 3:1 for isomesityl oxide: mesityl oxide is taken as an estimate based on uncertainty limits given from a fit of the photoionization spectra.

Several other significant peaks at 550 K are observed in the mass spectrum of Figure 1a. Those at m/z = 99 and 43 display rapid temporal onsets and do not decay precipitously as would be expected of a reactive radical. This kinetic behavior is in contrast to that of the stable products, which display more gradual temporal onsets. Alkylperoxy radicals do not typically have stable parent cations and are thus usually only detected as fragment ions.[42] The m/z = 99 peak in excess of the ^{13}C isotopologs from mesityl and isomesityl oxide might arise from dissociative ionization of one or more of the alkylperoxy radicals formed ($[RO_2]^+ \rightarrow [R]^+ + O_2$), and the m/z = 43 peak is also likely a fragment ion. The β-scission channels of R_{Tbu}, R_R, R_{Me}, and QOOH species can yield several small molecule products, including acetone (m/z = 58), isobutene (m/z = 56), ketene (m/z = 42), CO, and CH_3. A more detailed discussion, including figures, for these bond homolysis channels is given in the Supporting Information.

3.3. MTbuK Oxidation at 650 K. At 650 K, several changes from the 550 K case are observed in the oxidation spectra of MTbuK (Figure 1; Table 1). First, the peak at m/z = 56 (isobutene) becomes the dominant feature in the mass spectrum reflecting the greater degree of β-scission at higher temperature. Second, almost no acetone (m/z = 58) or cyclic ether product (m/z = 114) is seen. Finally, the shape of the photoionization spectrum of the m/z = 98 product attributed to HO_2-elimination changes, coming into better agreement with that of isomesityl oxide (Figure 2b). The assignment of isomesityl oxide is corroborated further by the agreement of the m/z = 43 and 83 photoionization spectra with the fragment ions of isomesityl oxide (see Supporting Information for further discussion). The emergence of isomesityl oxide at 650 K is

dx.doi.org/10.1021/ja405892y | J. Am. Chem. Soc. 2013, 135, 14256−14265

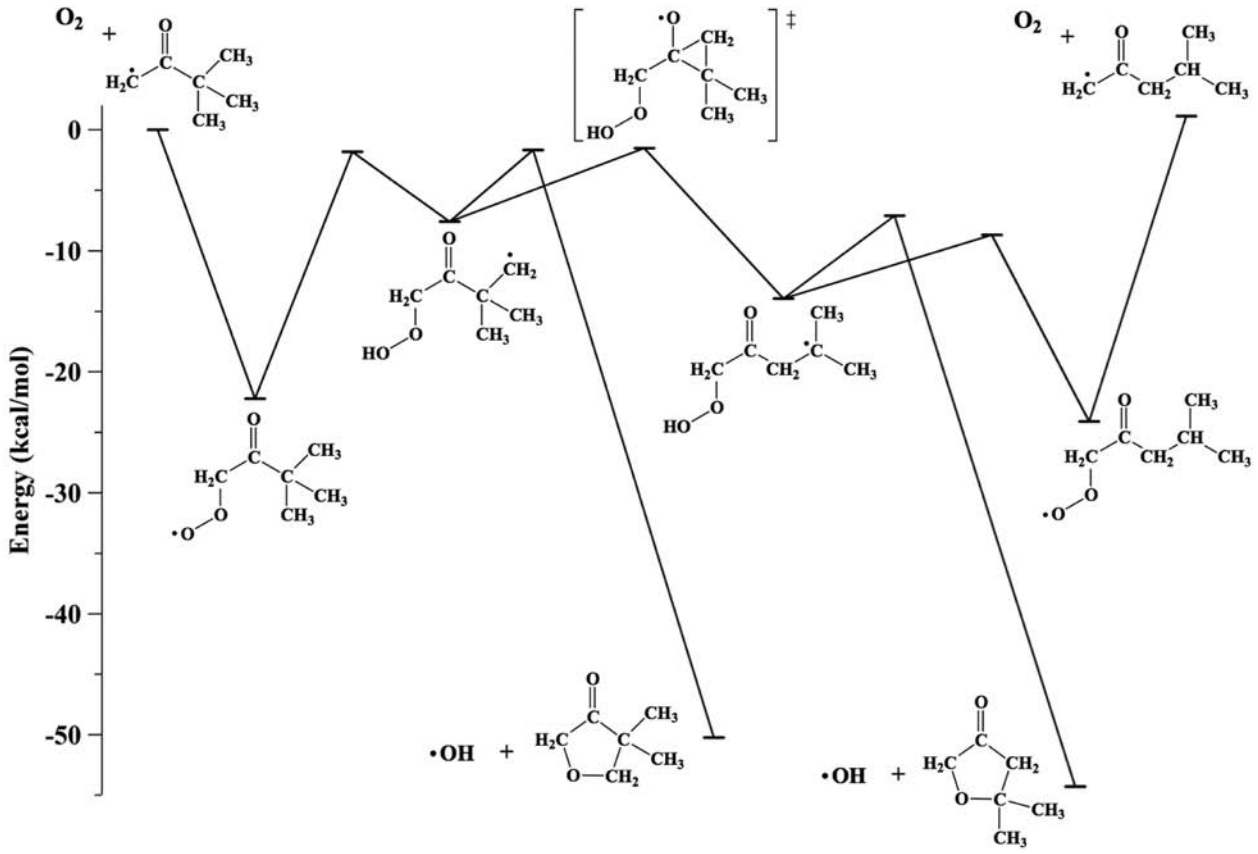

Figure 7. Stationary points on the potential energy surface for the reaction of the primary MTbuK radical R_{Me} with O_2. Energies at 0 K are at the CBS-QB3 level. Several β-scission channels are also possible but for clarity are not included.

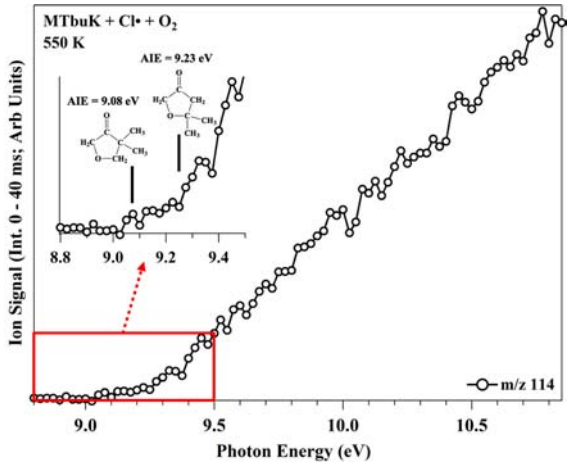

Figure 8. Photoionization spectrum of the m/z = 114 peak observed in Cl-initiated oxidation of MTbuK at 550 K. The inset shows ionization onset and calculated (CBS-QB3) AIEs for 4,4-dimethyl-tetrahydrofuran-3(2*H*)-one and 5,5-dimethyl-tetrahydrofuran-3(2*H*)-one.

somewhat surprising considering that at 550 K the photoionization spectra are consistent with >80% of the HO_2-elimination channel yielding the conjugated mesityl oxide isomer. At higher temperature, barriers for $RO_2 \rightarrow R(-H) + HO_2$ are more readily overcome for production of both mesityl and isomesityl oxide. It is possible that at 650 K the entropic favorability (3:1 ratio of primary to secondary H-atoms) of the isomesityl oxide channel dominates energetic effects that would favor mesityl oxide.

4. CONCLUSIONS

The 1,2-acyl migration in 3-oxoalkyl radicals, known to be facile in solution, is also rapid in the gas phase and will play an important role in developing accurate mechanisms and kinetics for the low-temperature oxidation of branched ketones. As demonstrated by a study of deuterated diethyl ketones, the rearrangement may take place even without a thermodynamic driving force provided by β substituents. Quantum chemical characterization of the saddle point for the 1,2-acyl group shift supports the reasoning of Karl et al.[15] and other calculations on Dowd−Beckwith rearrangements[18,19] that the configuration at the saddle point shows spin density at both the β and γ carbons relative to the O atom of the carbonyl group. No discrete cyclopropoxy radical intermediate is located when substituents at C_β provide a thermodynamic driving force for the reaction.

If the product of a 1,2-acyl rearrangement is more stable than the initial radical, such rearrangements are expected to be important even for parent molecules such as isopropyl ketones, in which bonding motifs allow traditional HO_2-elimination pathways without radical rearrangement. Characterization of fundamental oxidation chemistry is a key step toward predicting ignition behavior and identifying particular compounds as potentially useful liquid fuels. Future experimental and modeling efforts to describe the pyrolysis, oxidation, combustion, and ignition of branched ketones should address the gas phase 1,2-acyl group migration reactions described here. A detailed theoretical kinetics study both on the 1,2-acyl rearrangement and the O_2 addition reactions to the original and rearranged ketone radicals would be valuable, giving accurate gas-phase rate coefficients for these competing processes to be used in combustion models.

dx.doi.org/10.1021/ja405892y | J. Am. Chem. Soc. 2013, 135, 14256−14265

■ ASSOCIATED CONTENT

Supporting Information

Isomesityl oxide synthesis, analysis of the small-molecule products, fragment ions of mesityl and isomesityl oxide, absolute photoionization spectra for mesityl oxide, isomesityl oxide, 2,5-dimethylcyclopentanone, and 2,2,5,5-tetramethylcyclopentanone, absolute energies and Gaussian archive entries for all stationary points from Figures 3 and 7, Tables S1–S6, Figure S1–S5. This material is available free of charge via the Internet at http://pubs.acs.org.

■ AUTHOR INFORMATION

Corresponding Authors

amschee@sandia.gov

cataatj@sandia.gov

Notes

The authors declare no competing financial interest.

■ ACKNOWLEDGMENTS

The authors thank Prof. Barry Carpenter, Dr. Judit Zádor, and Dr. John D. Savee for useful discussions and Mr. Howard Johnsen for technical support of these experiments. We thank an anonymous reviewer for alerting us to the important work on the Dowd–Beckwith ring expansion. This work is supported by the Laboratory Directed Research and Development program at Sandia National Laboratories, a multiprogram laboratory operated by Sandia Corporation, a Lockheed Martin Company, for the United States Department of Energy (USDOE)'s National Nuclear Security Administration under contract DEAC04-94AL85000. The Advanced Light Source is supported by the Director, Office of Science, Office of Basic Energy Sciences, of the USDOE, under contract DE-AC02-05CH11231 between Lawrence Berkeley National Laboratory and the USDOE.

■ REFERENCES

(1) Scheer, A. M.; Mukarakate, C.; Robichaud, D. J.; Ellison, G. B.; Nimlos, M. R. *J. Phys. Chem. A* **2010**, *114*, 9043.
(2) Scheer, A. M.; Mukarakate, C.; Robichaud, D. J.; Nimlos, M. R.; Ellison, G. B. *J. Phys. Chem. A* **2011**, *115*, 13381.
(3) Lifshitz, A.; Tamburu, C.; Suslensky, A.; Dubnikova, F. *Proc. Combust. Inst.* **2005**, *30*, 1039.
(4) Fish, A. *Quarterly Reviews* **1964**, *18*, 243.
(5) Zador, J.; Taatjes, C. A.; Fernandes, R. X. *Prog. Energy Combust. Sci.* **2011**, *37*, 371.
(6) Beckwith, A. L. J.; Oshea, D. M.; Westwood, S. W. *J. Am. Chem. Soc.* **1988**, *110*, 2565.
(7) Tsai, A. I.; Chuang, C. P. *Tetrahedron* **2008**, *64*, 5098.
(8) Heusler, K.; Kalvoda, J. *Angew. Chem., Int. Ed.* **1964**, *3*, 525.
(9) Reusch, W.; Johnson, C. K.; Manner, J. A. *J. Am. Chem. Soc.* **1966**, *88*, 2803.
(10) Dowd, P.; Zhang, W. *Chem. Rev.* **1993**, *93*, 2091.
(11) Singh, S. K.; Strobel, G. A.; Knighton, B.; Geary, B.; Sears, J.; Ezra, D. *Microb. Ecol.* **2011**, *61*, 729.
(12) Strobel, G. A.; Knighton, B.; Kluck, K.; Ren, Y. H.; Livinghouse, T.; Griffin, M.; Spakowicz, D.; Sears, J. *Microbiology-(UK)* **2008**, *154*, 3319.
(13) Strobel, G. A.; Spang, S.; Kluck, K.; Hess, W. M.; Sears, J.; Livinghouse, T. *FEMS Microbiol. Lett.* **2008**, *283*, 140.
(14) Reimann, H.; Capomaggi, A. S.; Strauss, T.; Oliveto, E. P.; Barton, D. H. R. *J. Am . Chem. Soc.* **1961**, *83*, 4481.
(15) Karl, C. L.; Maas, E. J.; Reusch, W. *J. Org. Chem.* **1972**, *37*, 2834.
(16) Wang, Z. In *Comprehensive Organic Name Reactions and Reagents*; John Wiley and Sons: Hoboken, 2010; p 939.
(17) Dowd, P.; Choi, S.-C. *J. Am . Chem. Soc.* **1987**, *109*, 3493.
(18) Ryu, I.; Fukushima, H.; Okuda, T.; Matsu, K.; Kambe, N.; Sonoda, N.; Komatsu, M. *Synlett* **1997**, *11*, 1265.
(19) Ardura, D.; Sordo, T. L. *Tetrahedron Lett.* **2004**, *45*, 8691.
(20) Chatgilialoglu, C.; Timokhin, V. I.; Ballestri, M. *J. Org. Chem.* **1998**, *63*, 1327.
(21) Lindsay, D. A.; Lusztyk, J.; Ingold, K. U. *J. Am . Chem. Soc.* **1984**, *106*, 7087.
(22) Chatgilialoglu, C.; Ferreri, C.; Sommazzi, A. *J. Am . Chem. Soc.* **1996**, *118*, 7223.
(23) DeSain, J. D.; Klippenstein, S. J.; Taatjes, C. A. *Phys. Chem. Chem. Phys.* **2003**, *5*, 1584.
(24) Taatjes, C. A. *J. Combust. Soc. Jpn* **2008**, *50*, 29.
(25) Kaiser, E. W.; Wallington, T. J.; Hurley, M. D. *J. Phys. Chem. A* **2009**, *113*, 2424.
(26) Miller, J. A.; Klippenstein, S. J. *Int. J. Chem. Kinet.* **2001**, *33*, 654.
(27) Miller, J. A.; Klippenstein, S. J.; Robertson, S. H. *Proc. Combust. Inst.* **2000**, *28*, 1479.
(28) Wilke, J. J.; Allen, W. D.; Schaefer, H. F. *J. Chem. Phys.* **2008**, 128.
(29) Rienstra-Kiracofe, J. C.; Allen, W. D.; Schaefer, H. F. *J. Phys. Chem. A* **2000**, *104*, 9823.
(30) DeSain, J. D.; Klippenstein, S. J.; Miller, J. A.; Taatjes, C. A. *J. Phys. Chem. A* **2003**, *107*, 4415.
(31) Osborn, D. L.; Zou, P.; Johnsen, H.; Hayden, C. C.; Taatjes, C. A.; Knyazev, V. D.; North, S. W.; Peterka, D. S.; Ahmed, M.; Leone, S. R. *Rev. Sci. Instrum.* **2008**, *79*, 104103.
(32) Taatjes, C. A.; Hansen, N.; Osborn, D. L.; Kohse-Höinghaus, K.; Cool, T. A.; Westmoreland, P. R. *Phys. Chem. Chem. Phys.* **2008**, *10*, 20.
(33) Gillard, R. D.; Heaton, B. T.; Pilbrow, M. F. *J. Chem. Soc. A* **1970**, 353.
(34) Gillard, R. D.; Heaton, B. T.; Pilbrow, M. F. *Org. Prep. Proced. Int.* **1974**, *6*, 131.
(35) Montgomery, J. A.; Frisch, M. J.; Ochterski, J. W.; Petersson, G. A. *J. Chem. Phys.* **1999**, *110*, 2822.
(36) Montgomery, J. A.; Frisch, M. J.; Ochterski, J. W.; Petersson, G. A. *J. Chem. Phys.* **2000**, *112*, 6532.
(37) Welz, O.; Zádor, J.; Savee, J. D.; Ng, M. Y.; Meloni, G.; Fernandes, R. X.; Sheps, L.; Simmons, B. A.; Lee, T. S.; Osborn, D. L.; Taatjes, C. A. *Phys. Chem. Chem. Phys.* **2012**, *14*, 3112.
(38) Frisch, M. J.; Trucks, G. W.; Schlegel, H. B.; Scuseria, G. E.; Robb, M. A.; Cheeseman, J. R.; Scalmani, G.; Barone, V.; Mennucci, B.; Petersson, G. A.; Nakatsuji, H.; Caricato, M.; Li, X.; Hratchian, H. P.; Izmaylov, A. F.; Bloino, J.; Zheng, G.; Sonnenberg, J. L.; Hada, M.; Ehara, M.; Toyota, K.; Fukuda, R.; Hasegawa, J.; Ishida, M.; Nakajima, T.; Honda, Y.; Kitao, O.; Nakai, H.; Vreven, T.; Montgomery, J. A., Jr.; Peralta, J. E.; Ogliaro, F.; Bearpark, M.; Heyd, J. J.; Brothers, E.; Kudin, K. N.; Staroverov, V. N.; Kobayashi, R.; Normand, J.; Raghavachari, K.; Rendell, A.; Burant, J. C.; Iyengar, S. S.; Tomasi, J.; Cossi, M.; Rega, N.; Millam, N. J.; Klene, M.; Knox, J. E.; Cross, J. B.; Bakken, V.; Adamo, C.; Jaramillo, J.; Gomperts, R.; Stratmann, R. E.; Yazyev, O.; Austin, A. J.; Cammi, R.; Pomelli, C.; Ochterski, J. W.; Martin, R. L.; Morokuma, K.; Zakrzewski, V. G.; Voth, G. A.; Salvador, P.; Dannenberg, J. J.; Dapprich, S.; Daniels, A. D.; Farkas, Ö.; Foresman, J. B.; Ortiz, J. V.; Cioslowski, J.; Fox, D. J. *Gaussian 09*; Gaussian, Inc.: Wallingford CT, 2009.
(39) Lee, T. J.; Rendell, A. P.; Taylor, P. R. *J. Phys. Chem.* **1990**, *94*, 5463.
(40) Kaiser, E. W.; Wallington, T. J.; Hurley, M. D. *J. Phys. Chem. A* **2010**, *114*, 343.
(41) Estupinan, E. G.; Smith, J. D.; Tezaki, A.; Klippenstein, S. J.; Taatjes, C. A. *J. Phys. Chem. A* **2007**, *111*, 4015.
(42) Meloni, G.; Zou, P.; Klippenstein, S. J.; Ahmed, M.; Leone, S. R.; Taatjes, C. A.; Osborn, D. L. *J. Am. Chem. Soc.* **2006**, *128*, 13559.